Electrochimica Acta, Vol. 37, No. 7, pp. 1253–1260, 1992
Printed in Great Britain.

0013-4686/92 $5.00 + 0.00

MODIFICATION OF GRAPHITE ELECTRODE MATERIALS FOR VANADIUM REDOX FLOW BATTERY APPLICATION—I. THERMAL TREATMENT

B. SUN and M. SKYLLAS-KAZACOS*

School of Chemical Engineering and Industrial Chemistry, University of New South Wales, P.O. Box 1 Kensington, NSW 2033, Australia

(*Received* 10 *September* 1991)

Abstract—The thermal activation of graphite felt was investigated at a range of temperatures and treatment times so as to enhance the electrochemical performance of this material for use in the vanadium redox cell. Graphite felt treated thermally at 400°C exhibited the greatest improvement in performance of the vanadium cell. Energy efficiencies of over 88% were obtained after this treatment compared with only 78% for the untreated felt. Results from XPS analysis showed that surface functional groups of C—O and C = O increased dramatically compared with untreated samples, suggesting that these functional groups behave as active sites for the vanadium redox reactions.

Key words: graphite electrode, vanadium redox cell.

INTRODUCTION

The surface modification of graphite or carbon electrode materials has recently received a great deal of interest as it has become apparent that the nature of the surface functional groups can influence the electrocatalytic activity of this material[1–3]. Electrode modification can involve thermal, chemical or electrochemical treatments to improve the surface electrochemical activity.

Recent research has suggested that the oxygen functional groups on the carbon surface, behave as active sites for many electrochemical reactions[3–8]. For the vanadium redox cell reactions

$$V^{3+} + e \rightleftharpoons V^{2+} \quad (1)$$

and

$$VO_2^+ + 2H^+ + e \rightleftharpoons VO^{2+} + H_2O \quad (2)$$

it is likely that the redox couple reaction corresponding to the positive electrode in the vandium redox cell, $V^V \rightleftharpoons V^{IV}$ or equation (2) above, would be strongly influenced by the concentration and nature of the oxygen functional groups on the electrode surface, since oxygen transfer is involved.

The first observation of surface oxides on carbon was published by Smith[9] more than 100 years ago. He found that oxygen was chemisorbed by charcoal and could be recovered on heating only as carbon dioxide. Oxygen was bound by freshly outgassed charcoal even at −13°C and the gases evolved at 450°C consisted mainly of carbon monoxide[10]. Although Aschan had visualized in 1909 the correct structure made up from polycondensed aromatic nuclei[11], the structure of the carbon surface was not yet known at the time. Bartell and Miller[12–14] reported a series of observations on the adsorption of acid by sugar charcoals which had been activated at 800–1000°C by admittance of a limited supply of air. The anions were adsorbed and exchanged for hydroxide ions from neutral salt solutions.

Ogawa observed that carbon can acquire acid properties as well on oxidation. If it is heat treated and cooled in a high vacuum, it shows basic behaviour on admittance of molecular oxygen at room temperature[15]. However, if it is exposed to oxygen at moderate temperatures, *eg* 400°C, it turns acidic. By measuring the electrokinetic potentials, Kruyt and de Kadt found that the basic or acidic properties of the carbon sample depended on the temperature of reaction with oxygen[16]. Cookson also reported that acidic surface oxides are formed when the carbon is exposed to oxygen at temperatures between 200 and 500°C[32]. Basic surface oxides, on the other hand, are formed when a carbon surface is freed from all surface oxides by heating in a vacuum or in an inert atmosphere, and then brought in contact with oxygen only after cooling to low temperatures.

Shilov[19] formulated the acidic surface oxides as carboxylic acid anhydrides bound to the edges of the carbon layers. King[20] found that the acidic surface oxides were formed when carbon was treated with oxygen near its ignition point temperature and the maximum amount of acidic groups formed at 420°C. It was found that the reaction of oxygen with microcrystalline carbon at 400–450°C yields four groups of different acidities: a more strongly acidic carboxyl group (I), a more weakly acidic carboxyl group (II) as hydroxy lactone, a phenolic hydroxyl group (III), and carbonyl[21].

Smith and co-workers[22] also studied the reaction of oxygen with carbon between 250 and 450°C. From *ir* spectra, they showed the presence of lactone and carbonyl structures on the surface of carbon after exposure to oxygen.

*Author to whom correspondence should be addressed.

Hart *et al.*[23] studied the chemisorption of oxygen on well-cleaned carbon surfaces at different temperatures from 25 to 400°C with an oxygen pressure of 500 milliTorr. These studies illustrated that chemisorption from 25 to 250°C involves only one type of site, and that chemisorption above 300°C involves two types of sites. Hart *et al.* concluded that the oxygen adsorbed at 250°C primarily involved the formation of lactone groups with carbon fragments, and that the oxygen adsorbed at temperatures above 300°C primarily involved the formation of carbonyl groups at conventional "arm chair" and/or zig-zag carbon configurations.

The acidic groups were also produced by baking spectroscopic grade graphite rods in air at 160°C for 36 h[24]. Walker and co-workers also studied chemisorption of oxygen in the temperature range of 300–625°C at low pressure up to 0.5 mmHg on Graphon, a highly graphitized carbon black which was previously oxidized to different burn-offs in oxygen at 625°C, so as to introduce significant amounts of active surface area. A sharp increase in the saturation amount of oxygen adsorbed at a temperature of about 400°C was observed. This suggested the presence of two types of active sites[25–28].

When active charcoal reacts with oxygen at a temperature as low as 300°C, part of the oxygen consumed remains bound to the surface, being liberated as CO and CO_2 only on subsequent heating[29, 30].

In this study, the thermal treatment of graphite felt has been investigated at various temperatures and treatment times in order to improve the surface activity of the electrode material for the vanadium redox reactions by increasing the concentration of oxygen groups on the surface of the carbon.

EXPERIMENTAL

Samples of 3-mm thick graphite felt (Fibre, Material Inc., U.S.A.) were treated thermally in air atmospheres at various temperatures from 200° to 500°C for 30 h, and were also activated at constant temperature of 400°C for various times from 10 to 50 h. After the treatment at higher temperatures, the samples were cooled down in air before being used for various measurements.

To evaluate the electrochemical properties of the electrode material for the vanadium battery applications, a polarization test was conducted in the test flow cell illustrated in Fig. 1. The redox test flow cell, a *dc* power supply, two multimeters and a resistor of 1 Ω were employed for the polarization tests, this being the same as the equipment used in charge–discharge experiments. The electrolytes employed in each half cell corresponded to 50% state-of-charge (SOC) solutions, *ie* 1 M V^{II} + 1 M V^{III}/2.5 M H_2SO_4 solution as the negative electrolyte, and 1 M V^{IV} + 1 M V^{V}/3.5 M H_2SO_4 solution as the positive electroloyte. The cell was charged for 1 min at a constant current density within the range from 25 to 75 mA cm^{-2}. After a 15 s rest interval, the cell was discharged for 1 min at the same current density as that used for charging. The above procedure was repeated at various current densities to obtain plots

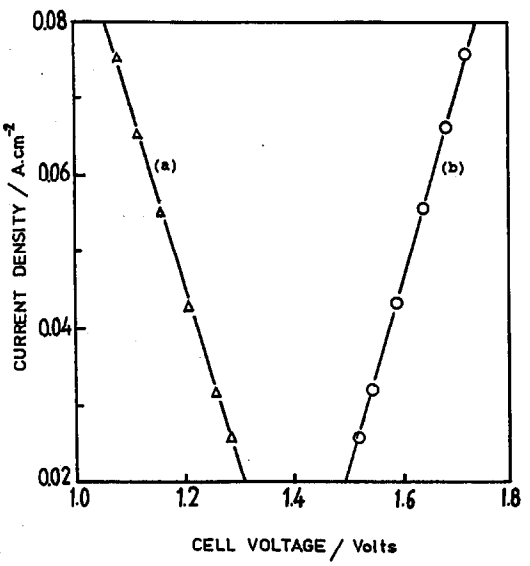

Fig. 1. Polarization curves of charge–discharge of vanadium redox cell using untreated graphite felt (3-mm thickness), 2 M $V^{2.5+}$/2.5 M H_2SO_4 as positive electrolyte and 2 M $V^{4.5+}$/3.5 M H_2SO_4 as negative electrolytes, respectively.

of current versus voltage for the charge and discharge cycle. From the slopes of these *I–V* plots, values of the cell resistance could be calculated for the charge and discharge processes.

The charge–discharge test apparatus employed was the same as for the cell resistance measurements. 2 M V^{4+}/3 M H_2SO_4 and 2 M V^{3+}/2 M H_2SO_4 solutions were used as the positive and negative electrolytes, respectively. Constant current densities of 25, 40 and 60 mA cm^{-2} were employed for charging and discharging.

Equal volumes of a solution containing a 50:50 mixture of V^{III} and V^{IV} in 2.5 M H_2SO_4 were initially placed into each half of vanadium redox cell to generate the positive (V^{V}) and negative (V^{II}) fully charged electrolytes from an initial charging cycle involving 1.5 equivalents per mole of vanadium ion. The voltage and current was also recorded as a function of time on a two-pen chart recorder. The cell charge and discharge cycles were controlled automatically and continuously by an Automatic Battery Cycling controller between set upper and lower voltage limits. From the resultant charge–discharge curves the cell coulombic, voltage and overall energy efficiencies were determined by calculations of current, time required and average cell voltage. All cell measurements were conducted at room temperature.

Scanning Electron Microscopy (SEM) was performed on a JEOL JXA-840 SEM within the School of Materials Science. X-Ray photoelectron Spectroscopy (XPS) was carried out at the Surface Analytical Center of the Chemistry Department of Queensland University.

RESULTS AND DISCUSSION

The surface wetting properties of the graphite felt were initially studied in acidic vanadium solution. In

the present study the hydrophilicity of the graphite felt was measured by visually examining the wetting condition of the graphite felt in 2 M $VOSO_4$ + 2 M H_2SO_4 solution.

It was observed that the clean graphite felt surface is hydrophobic. The time for untreated graphite felt to show signs of wetting in 2 M $VOSO_4$/2 M H_2SO_4 solution was 52 days. However, the wetting properties of the graphite felt improved after activation of the samples. The hydrophilicity of the graphite material improved after thermal treatment and increased dramatically when the treatment temperature was increased as seen as in Table 1. The reason for the improvement in the hydrophilic property is believed to be due to the formation of surface oxides which provide adsorption sites for water and other polar compounds, as previously reported[17]. The amount of surface oxides is affected by the treatment temperature and time.

The activity of the graphite felt electrode in the vanadium redox flow cell was also found to increase dramatically after thermal treatment.

Polarization curves for untreated graphite felt in the vanadium redox battery were obtained by plotting applied current (I) vs. cell voltage (V), for the discharge and charge cycle and are shown in Fig. 1, curves (a) and (b) respectively. The cell resistance values calculated from the slopes of the lines, were 4.09 and 4.22 Ω cm^2 for charge and discharge, respectively.

From such polarization curves it is possible to estimate the variation in activity of the electrode material. The cell resistance values obtained from the slope reflect the resistance to electron transfer (the ohmic resistance being constant) since the same cell is used for each electrode sample. The ratio of the discharge cell voltage to the charge cell voltage is also a measure of the cell voltage efficiency since 50% SOC electrolytes were employed in the measurement.

According to this method, the cell voltage efficiency can be determined at any current density simply by reading the appropriate voltages from the polarization curves. The total cell voltage for charging and discharging is given by

$$V_{ch} = E^0 + iR + \eta_{act} + \eta_{conc} \quad (3)$$

and

$$V_{disch} = E^0 + iR + \eta_{act} + \eta_{conc}, \quad (4)$$

where E^0 is the equilibrium potential, i, the current, R, the ohmic resistance, η_{act}, the activation overpotential, and η_{conc}, the concentration overpotential.

Table 1. The wetting properties of graphite felt samples in 2 M $VOSO_4$/2 M H_2SO_4 solution

Treatment condition of the sample	Time to start wetting/days
Untreated	52
200°C for 30 h	30
300°C for 30 h	Immediately (partially)
400°C for 10 h	Immediately (partially)
400°C for 20 h	Immediately
400°C for 30 h	Immediately
400°C for 50 h	Immedatiely
500°C for 30 h	Immediately

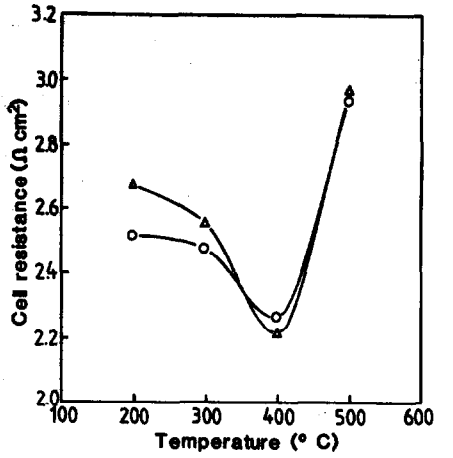

Fig. 2. Effect of treatment temperature on the cell resistance for activated graphite felt, (○) charge and (△) discharge.

As long as the same cells, electrolytes, flowrates and temperatures are employed in all tests, the magnitude of E^0, iR and η_{conc} should always remain the same. Any variations in the measured values of V_{ch}, V_{disch} and cell resistance should thus reflect changes in the activation overpotential (η_{act}) at the positive and/or negative electrodes, which is, in turn, a measure of the electrochemical activity of the electrode.

The effect of treatment temperature on the cell resistance for thermally activated graphite felt in the vanadium redox flow cell is shown in Fig. 2. As mentioned earlier the values of the cell resistance obtained with untreated felt were 4.09 and 4.22 Ω cm^2 for charge and discharge, respectively. After thermal treatment, however, the cell resistance is seen in Fig. 2 to drop initially with increasing activation temperature, reaching a minimum value at 400°C. At higher temperatures the cell resistance is seen to increase dramatically for the constant treatment time of 30 h.

The effect of treatment time at constant temperature on the cell resistance is illustrated in Fig. 3. The minimum value obtained at an activation time of 30 h at approximately 400°C makes this the most suitable time for this graphite material. For shorter or longer treatment times, the graphite felt exhibited a lower activity in the vanadium redox cell.

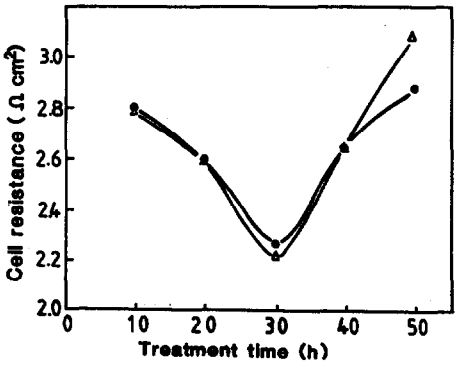

Fig. 3. Effect of activation time on the cell resistance at constant tempertaure of 400°C for graphite felt, (○) charge and (△) discharge.

Results from charge–discharge cycling in the vanadium redox cell can give additional important information on the activity of the graphite felt electrodes since the coulombic efficiency determined gives a measure of the selectivity of the electrode for the vanadium redox reactions. As long as the cell geometry and membrane are kept the same for all tests, any changes in coulombic efficiency will reflect changes in electrode selectivity (for the vanadium *vs* decomposition reactions) with treatment, which will in turn affect the overall energy efficiency of the cell. Cell efficiency measurements for untreated and activated samples were therefore carried out by charge–discharge cycling of the vanadium redox test flow cell.

A typical charge and discharge curve for a vanadium redox cell employing graphite felt thermally activated at 400°C for 30 h is shown in Fig. 4. The charge and discharge were performed at a constant current density of 25 mA cm^{-2}. The coulombic, voltage and overall energy efficiency values for 90 charge–discharge cycles at 25, 40 and 60 mA cm^{-2} are summarized in Table 2. Increasing the current density is seen to decrease the cell voltage efficiency as expected, due to increased *iR* losses. At higher current densities the coulombic efficiency increases, however, due to the lower self-discharge across the membrane in the shorter cycle time. Comparing these values with charge–discharge results for an untreated sample which are shown in Table 3, significant improvements in both coulombic and voltage efficiencies show as a result of thermal activation of the graphite felt.

The higher voltage efficiency values obtained with the treated felt are consistent with the cell resistance measurements reported above. The average coulombic efficiency at a current density of 25 mA cm^{-2} is 95.6% after treatment, with a voltage efficiency of 92.0%, and overall energy efficiency of 88.0% for the first 10 cycles. When the current density was increased to 40 mA cm^{-2} from the eleventh to fiftieth cycle, the average values of coulombic, voltage and energy efficiencies were 98.2, 87.2 and 85.6%, respectively, again significantly higher than for the untreated felt. Furthermore, the voltage efficiency still remained high at a value of 83.0% even at a current density of 60 mA cm^{-2} and after a total of 90 cycles.

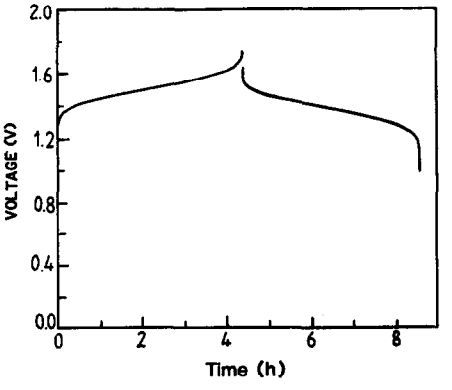

Fig. 4. Charge–discharge curves (10th cycle) for vanadium redox cell employing graphite felt activated at 400°C for 30 h. Charge–discharge current density is 25 mA cm^{-2}.

Table 2. Vanadium redox cell efficiencies for graphite felt electrode treated at 400°C for 30 h

Current density/ mA cm^{-2}	Cycle number	Cell efficiency/% η_c	η_v	η_E
25	1	95.0	92.6	88.0
	5	95.8	91.0	87.2
	10	96.0	91.8	88.1
	Average	95.6	91.8	87.8
40	11	97.6	87.0	84.9
	15	96.8	86.7	83.9
	20	98.8	86.9	85.9
	25	99.1	87.0	86.3
	30	96.2	86.0	82.7
	35	98.3	87.8	86.3
	40	99.1	88.2	87.4
	45	99.1	87.6	86.8
	50	99.1	87.9	87.1
	Average	98.2	87.2	86.0
60	51	98.6	82.8	81.6
	55	95.3	82.9	79.0
	60	97.2	82.8	80.5
	65	97.1	82.9	80.5
	70	97.1	82.9	80.5
	75	98.3	82.8	81.4
	80	96.7	82.9	80.2
	85	98.3	83.4	80.0
	90	97.2	83.4	81.1
	Average	97.3	83.0	80.8

In order to investigate the surface morphology of the thermally activated graphite felt material in the vanadium species reactions, scanning electron microscopy (SEM) and X-ray photoelectron spectroscopy (XPS) were employed in this study.

The surface morphology of the graphite felt both before and after thermal treatment at 400°C is illustrated in the SEMs of Figs 5 and 6. From these photographs it is seen that there is not much difference in the surface condition of the activated and untreated samples, *ie* the physical state of the surface of the graphite felt after thermal activation does not appear to have changed.

The results from XPS measurements are shown in Figs 7 and 8, which are general surveys for the surfaces of thermally activated and untreated graphite felt samples, respectively. It can be noted that the amount of chemisorbed oxygen on the activated

Table 3. Cell efficiencies for untreated graphite felt electrode in vanadium test flow cell

Current density/ mA cm^{-2}	Cycle number	Cell efficiency/% η_c	η_v	η_E
25	1	93.2	84.5	78.7
	2	92.6	85.9	79.5
	3	91.6	85.4	78.2
40	4	96.0	77.3	74.3
	5	97.0	76.5	74.3
	6	94.2	76.2	71.4
60	7	97.0	68.2	66.2
	8	96.9	67.9	65.8
	9	96.9	67.5	65.4

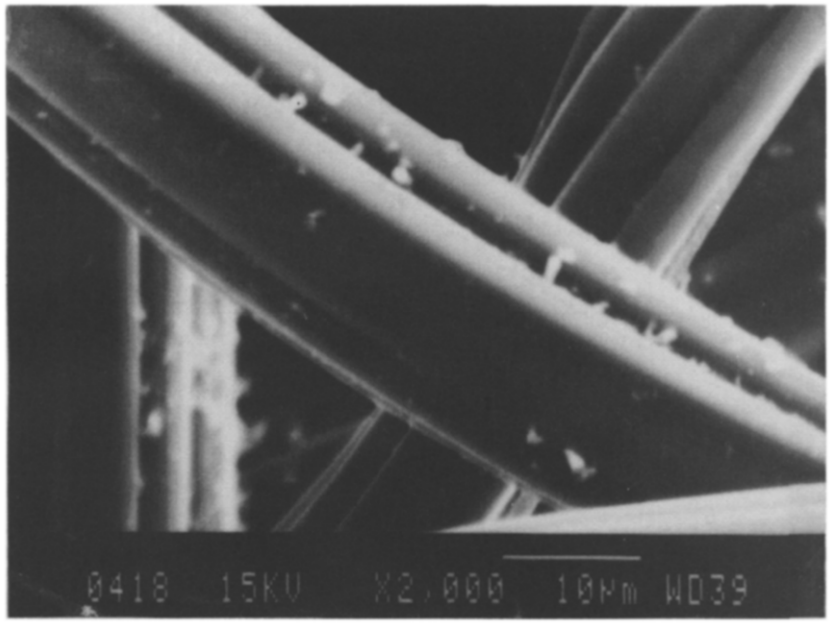

Fig. 5. The surface morphology of graphite felt.

graphite felt surface has increased dramatically. The atomic O/C ratio increased from 0.0379 for untreated to 0.200 for activated sample. Curve fittings of the O1*s* for both samples are shown in Figs 9 and 10. It can be seen that deconvolution of the oxygen peak using the curve fitting routine shows two functional groups, namely C—O and C = O on the graphite felt surface. For the thermally activated sample, the ratio of C—O and C = O is approximately 2:1, and the amount of C—O is also four times higher than that of the untreated felt. The functional groups containing C—O are believed normally to be phenolic groups and those associated with C = O are carboxylic groups, as previously reported[21]. The C = O is also believed to be associated with carbonyl groups[23]. The increased activity of the thermally treated graphite felt for the vanadium redox reactions can thus be attributed to the increased surface concentration of the functional groups of C—O and C = O produced during activation. The C—O groups on the electrode surface probably behave as active sites, catalysing the vanadium species reactions. The mechanism of catalysis for reactions on the electrode surface can be hypothesized as follows.

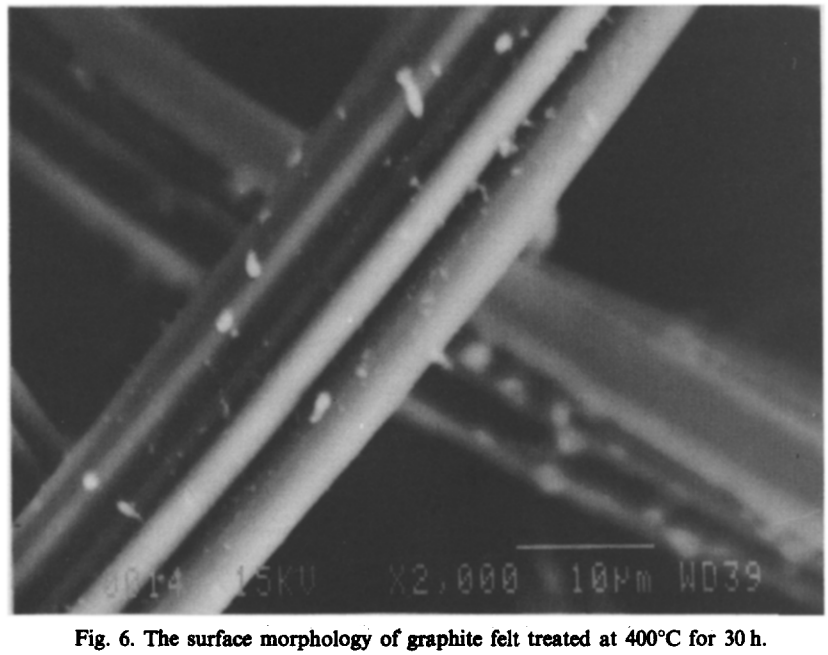

Fig. 6. The surface morphology of graphite felt treated at 400°C for 30 h.

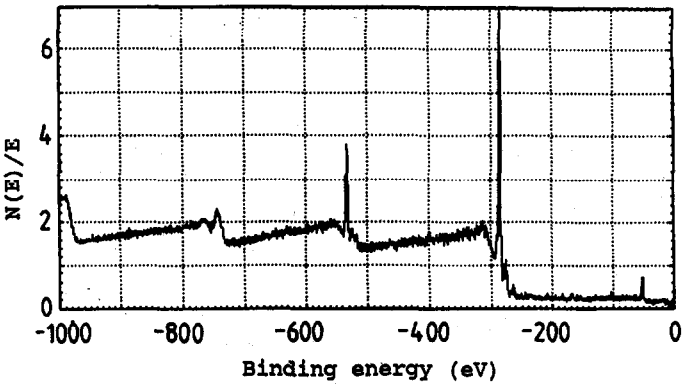

Fig. 7. General XPS survey of major elements for graphite felt thermally activated at 400°C.

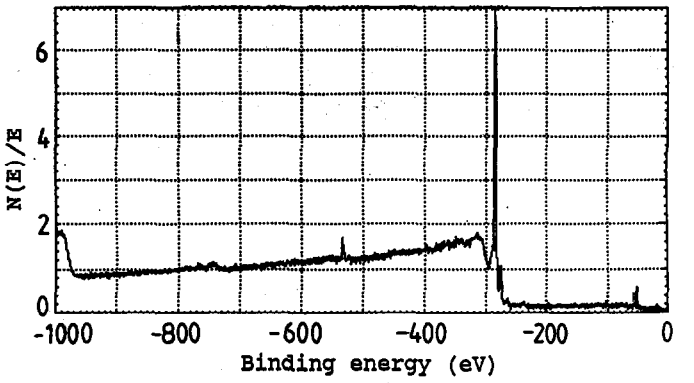

Fig. 8. General XPS survey of major elements for untreated graphite felt.

In the positive half-cell, the reactions occur as

$$VO^{2+} + H_2O \underset{\text{discharge}}{\overset{\text{charge}}{\rightleftharpoons}} VO_2^+ + 2H^+ + e. \quad (5)$$

As can be seen from this reaction, the charge and discharge processes at the positive electrode involve the transfer of an oxygen atom, which is likely to be the rate determining step in the overall mechanism. The availability of oxygen groups on the electrode surface would thus be expected to affect the overall rate of the reactions. Thus, during charge the following processes occur.

(a) The first step involves the transport of VO^{2+} ions from the bulk of the solution to the electrode surface and ion-exchange with hydrogen ions of the phenolic functional groups on the graphite surface thus bonding onto the electrode surface, as shown below:

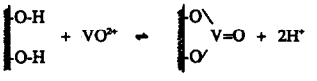

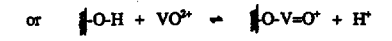

(6)

(b) In the second step, electron transfer occurs from the VO^{2+} to the electrode along the —C—O—V— bond as well as the transfer of one of the oxygen

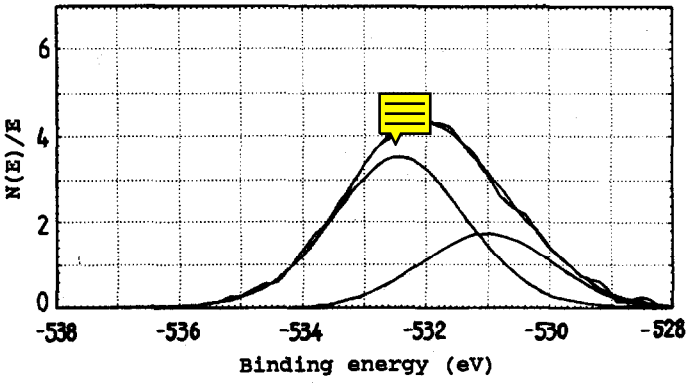

Fig. 9. Curve fitting of the O1*s* from the surface of graphite felt thermally activated at 400°C for 30 h.

532.5 531

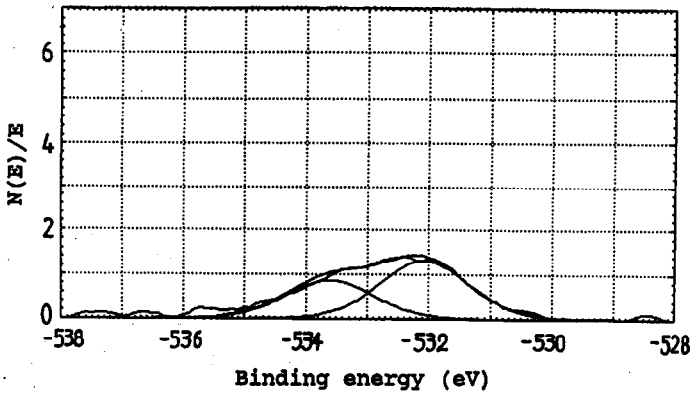

Fig. 10. Curve fitting of the O1s from the surface of untreated graphite felt.

atoms on the C—O functional group to the VO^{2+} forming a surface VO_2^+:

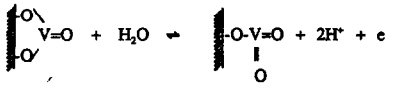

or 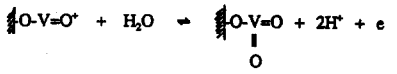 (7)

(c) Finally, the VO_2^+ exchanges with a H^+ from solution and diffuses back into the bulk solution:

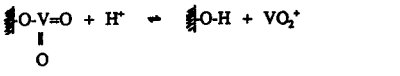 (8)

From the above hypothetical reaction sequence for the charge process involving the V^{IV}/V^V redox couple, it can be seen that electron transfer reaction can be accelerated along the —C—O—V— bond, and oxygen transfer from the C—O—H functional group will also be easier than directly from H_2O. The rate of the overall process would thus be increased leading to reduced activation overpotential and increased cell efficiencies.

For the discharge process, the reverse reactions would occur, although the steric hindrance associated with the more bulky VO_2^+ ion attaching itself to a surface —C—O group would make this process more difficult than the charge process and would explain the higher activation overvoltage often observed for the $V^V \rightarrow V^{IV}$ reaction in cyclic voltammetry[31].

We can thus conclude that the functional group, C—OH, catalyses the VO_2^+/VO^{2+} redox reaction, by producing active sites for the reactions. The higher the surface concentration of the C—OH functional groups produced on the electrode surface, the higher the activity obtained for the vanadium species reactions.

The variation in the activity of the graphite felt with treatment conditions is thus associated with the concentration of the functional groups produced on the electrode surface. Boehm[17] reported that surface oxides were already formed at 200°C. Cookson also announced that acidic surface oxides are formed when carbon is exposed to oxygen at temperatures between 200 and 500°C[32]. The maximum amount of chemisorb oxygen on the surface was found at around 400°C in the present study and is consistent with that previously reported[15, 19, 25–28]. When the temperature was increased to 500°C, the activity of the graphite felt was reduced. This is believed to be due to the decomposition of the surface oxygen functional groups with the evolution of carbon dioxide or carbon monoxide and a decrease in the surface concentration of the functional groups.

Weight loss measurements of graphite felt after thermal treatment are illustrated in Fig. 11. It can be seen that the burn off of graphite felt increases with increasing temperature. Notably, when the temperature is increased from 400 to 500°C, a dramatic increase in weight loss of the material from 1.07 to 11.02% is obtained. The results from this study are consistent with previous reports by Boehm[17] who noted that at elevated temperature, the oxidized graphite evolved molecular oxygen as well as CO and CO_2, and the surface complex was decomposed by the evolution of carbon dioxide at 500°C. For thermal activation of graphite materials, the optimum temperature for the development of maximal capacity to absorb base has been shown to lie close to 400°C. This temperature is also the optimum temperature for maximum fixation of oxygen [29].

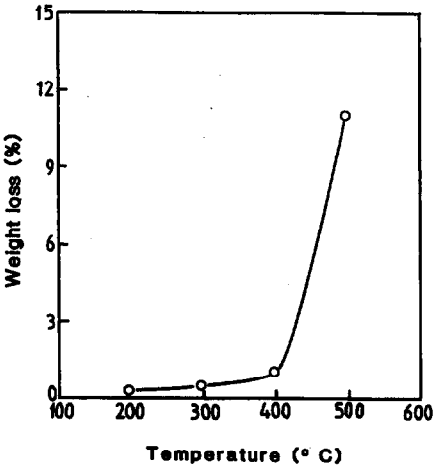

Fig. 11. Variation of weight loss for graphite felt with activation temperature (treatment time: 30 h).

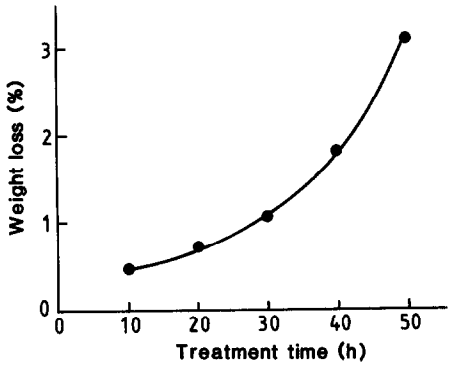

Fig. 12. Effect of treatment time on weight loss for the graphite felt activated at 400°C.

The effect of treatment time on measured weight loss of graphite material at a constant temperature of 400°C is shown in Fig. 12. The burn off of the samples is thus also increased by prolonged treatment time, although the influence of time on weight change is only slight, and is consistent with the results from cell resistance measurements.

CONCLUSIONS

Thermal activation has been employed in this study for optimization of the electrochemical activity of graphite felt. The improved activity of the graphite felt activated at 400°C for 30 h has led to a significant improvement in vanadium redox cell efficiencies and to the lowest cell resistance values. Energy efficiencies of over 88% were obtained after treatment compared with only 78% for the untreated felt. The increase in the activity of this material is attributed to the formation of surface active functional groups of C—O—H and C = O as confirmed by XPS analysis. A reaction sequence for charge and discharge processes at the positive electrode of a vanadium redox cell has been proposed. This involves formation of a —C—O—V bond which facilitates the electron transfer and oxygen transfer processes and thus reduces the activation overpotential for the V^{IV}/V^{V} redox reactions.

Acknowledgements—This project has been funded by the Australian National Energy Research Development and Demonstration Council and the NSW Department of Minerals and Energy.

REFERENCES

1. M. Poon, R. L. McCreery and R. Engstrom, *Anal. Chem.* **60**, 1725 (1988).
2. L. J. Kepley and A. J. Bard, *Anal. Chem.* **60**, 1459 (1988).
3. R. C. Engstrom and V. A. Strasser, *Anal. Chem.* **56**, 136 (1984).
4. C. Amatore, J. M. Saveant and D. Tesser, *J. electroanal. Chem.* **146**, 37 (1983).
5. R. W. Wightman, M. R. Deakin, P. M. Kovach, W. G. Kuhr and K. J. Stutts, *J. electrochem. Soc.* **131**, 1578 (1984).
6. N. Cenas, J. Rozgaite, A. Pocus and J. Kulys, *J. electroanal. Chem.* **154**, 121 (1983).
7. G. N. Kamau, W. S. Willis and J. F. Rusling, *Anal. Chem.* **57**, 545 (1985).
8. J. F. Evans, T. Kuwana, M. T. Henne and C. P. Royer, *J. electroanal. Chem.* **80**, 409 (1977).
9. A. Smith, *Proc. Roy. Soc.* **A12**, 424 (1863); *Ann. Chem. Pharm. Suppl.* **2**, 262 (1863).
10. C. J. Baker, *Chem. Soc.* **51**, 249 (1887).
11. O. Aschan, *Chem. Ztg* **33**, 561 (1909).
12. F. E. Bartell and E. J. Miller, *J. Am. chem. Soc.* **44**, 1866 (1922); **45**, 1106 (1923).
13. E. J. Miller, *J. Am. chem. Soc.* **46**, 1150 (1924); **46**, 1270 (1925).
14. E. J. Miller, *J. phys. Chem.* **30**, 1031–1162 (1926); **31**, 1197 (1927).
15. I. Ogawa, *Biochem. Z.* **172**, 249 (1926).
16. H. R. Kruyt and G. S. de Kadt, *Kolloid-Z* **47**, 44 (1929).
17. H. P. Boehm, *Chemical Identification of Surface Groups*, Advances in Catalysis 16: 179 (Edited by D. D. Eley, H. Pires and P. B. Weisz). Academic Press, New York (1966).
18. N. Shilov, H. Shatonovskaya and K. Chmutov, *Z. Physik. Chim. (Leipzig)* **A 149**, 211 (1930).
19. N. Shilov, *Kolloid-Z* **52**, 107 (1930).
20. A. King, *J. chem. Soc.* 1489 (1937).
21. H. P. Boehm, E. Diehl, W. Heck and R. Sappok, *Angew. Chem. Internatn. Edn*, **3** (10), 669 (1964).
22. R. N. Smith, D. A. Young and R. A. Smith, *Infrared Study of Carbon–Oxygen Surface Complexes, Trans. Faraday Soc.* **62**, 2280 (1966).
23. P. L. Hart, F. J. Vastola and P. L. Walker, Jr, *Carbon* **3**, 363 (1967).
24. B. F. Watkins, J. R. Behling, E. Kariv and L. L. Miller, *J. Am. chem. Soc.* **97**, 3549 (1975).
25. N. R. Laine, F. J. Vastola and P. L. Walker, Jr, *J. phys. Chem.* **67**, 2030 (1963).
26. N. R. Laine, F. J. Vastola and P. L. Walker, Jr, *Proc. Fifth Conf. on Carbon*, Penn. State, 1961, Vol. **11**, p. 211. Pergamon Press, New York (1963).
27. P. J. Hart, F. J. Vastola and P. L. Walker, Jr, *Carbon* **5**, 363 (1967).
28. R. O. Lussow, F. J. Vastola and P. L. Walker, Jr, *Carbon* **5**, 591 (1967).
29. T. F. E. Read and R. V. Wheeler, *J. chem. Soc. (London)* **13**, 461 (1913).
30. B. R. Puri, D. D. Singh, J. Nath and L. R. Sharma, *Ind. Eng. Chem.* **50**, 1071 (1958).
31. E. Sum, M. Rychcik and M. Skyllas-Kazacos, *J. Pwr Sources* **19**, 45 (1987).
32. J. T. Cookson, Jr, *Carbon Adsorption Handbook* (Edited by P. N. Cheremisinoff), p. 241. Ann Arbor Science (1978).